



## 1    **Variability of Black Carbon mass concentration in surface snow at Svalbard**

2    Michele Bertò<sup>1#</sup>, David Cappelletti<sup>2,7</sup>, Elena Barbaro<sup>1,3</sup>, Cristiano Varin<sup>1</sup>, Jean-Charles Gallet<sup>4</sup>, Krzysztof  
3    Markowicz<sup>5</sup>, Anna Rozwadowska<sup>6</sup>, Mauro Mazzola<sup>7</sup>, Stefano Crocchianti<sup>2</sup>, Luisa Poto<sup>1,3</sup>, Paolo Laj<sup>8</sup>,  
4    Carlo Barbante<sup>1,3</sup> and Andrea Spolaor<sup>1,2\*</sup>.

5  
6    <sup>1</sup>Ca' Foscari University of Venice, Dept. Environmental Sciences, Informatics and Statistics, via Torino,  
7    155 - 30172 Venice-Mestre, Italy;

8    <sup>2</sup>Università degli Studi di Perugia, Dipartimento di Chimica, Biologia e Biotecnologie, Perugia, Italy;

9    <sup>3</sup>CNR-ISP, Institute of Polar Science – National Research Council –via Torino, 155 - 30172 Venice-  
10    Mestre, Italy;

11    <sup>4</sup>Norwegian Polar Institute, Tromsø, Norway.

12    <sup>5</sup>University of Warsaw, Institute of Geophysics, Warsaw, Poland;

13    <sup>6</sup>Institute of Oceanology, Polish Academy of Sciences, Sopot, Poland;

14    <sup>7</sup>CNR-ISP, Institute of Polar Science – National Research Council – Via Gobetti 101, Bologna;

15    <sup>8</sup>Univ. Grenoble-Alpes, CNRS, IRD, Grenoble-INP, IGE, 38000 Grenoble, France

16  
17    <sup>#</sup> Now at Laboratory of Atmospheric Chemistry, Paul Scherrer Institute, 5232 Villigen PSI, Switzerland

18  
19    Correspond to: Andrea Spolaor, [andrea.spolaor@cnr.it](mailto:andrea.spolaor@cnr.it); Michele Bertò, [michele.berto@gmail.it](mailto:michele.berto@gmail.it)

## 21    **Abstract**

22        Black Carbon (BC) is a significant forcing agent in the Arctic, but substantial uncertainty remains  
23    to quantify its climate effects due to the complexity of the different mechanisms involved, in particular  
24    related to processes in the snow-pack after deposition. In this study, we provide detailed and unique  
25    information on the evolution and variability of BC content in the upper surface snow layer during the  
26    spring period in Svalbard (Ny-Ålesund). Two different snow-sampling strategies were adopted during  
27    spring 2014 and 2015, providing the *refractory* BC (rBC) mass concentration variability on a  
28    seasonal/daily and daily/hourly time scales. The present work aims to identify which atmospheric  
29    variables could interact and modify the mass concentration of BC in the upper snowpack, the snow layer  
30    which BC particles affects the snow albedo. Atmospheric, meteorological, and snow-related physico-  
31    chemical parameters were considered in a multiple linear regression model to identify the factors that  
32    could explain the variations of BC mass concentrations during the observation period. Precipitation



33 events were the main drivers of the BC variability. Snow metamorphism and activation of local sources  
34 during the snow melting periods appeared to play a non-negligible role (wind resuspension in specific  
35 Arctic areas where coal mines were present). The statistical analysis suggests that the BC content in the  
36 snow is decoupled from the atmospheric BC load.

## 37 1. Introduction

38 In the last two decades, the Arctic region has been exposed to dramatic changes in terms of  
39 atmospheric temperature rise, sea ice decrease, and increase of air mass transport from lower latitudes  
40 bringing warmer and humid air masses containing pollutants and anthropogenic derived compounds (Law  
41 and Stohl, 2007; Comiso et al., 2008; Screen and Simmonds, 2010; Eckhardt et al., 2013; Schmale et al.,  
42 2018; Maturilli et al., 2019). Long-range transport and local emissions of combustion generating aerosols  
43 like black carbon (BC) can influence the radiative budget of the Arctic atmosphere, especially the  
44 impacts of atmospheric aging on the mixing state of BC particles (Eleftheriadis et al., 2009; Bond et al.,  
45 2013; Zanatta et al., 2018). When deposited over snow, numerous aerosol species directly increase the  
46 quantity of solar radiation absorbed by the snowpack, thus favouring snow aging processes and the  
47 decrease of the snow albedo (Hansen and Nazarenko, 2004; Flanner et al., 2007; Hadley and Kirchstetter,  
48 2012; Skiles et al., 2018; Skiles and Painter, 2019).

49 Among these light-absorbing aerosols, *black carbon* (BC) particles are the most effective in  
50 absorbing the visible and near infrared solar radiation. These primarily emitted, insoluble, refractory and  
51 carbonaceous particles originate from natural and anthropogenic sources such as open fires or diesel  
52 engine exhausts. Currently, the anthropogenic emissions are higher compared to the natural ones  
53 (Moosmüller et al., 2009; Bond et al., 2013). In 2000 the energy production sector (including fossil fuels  
54 and solid residential fuels combustion) generated approximately 59% of the total global BC emissions  
55 while the remaining came from biomass burning (Bond et al., 2013). BC particles are characterized by a  
56 mass size distribution peaking around 100-250 nm (or mass equivalent diameter), e.g. 240 nm in the  
57 Svalbard area in spring (Bond et al., 2013; Laborde et al., 2013; Zanatta et al., 2016; Motos et al., 2019).  
58 The impact of BC particles absorbing the incoming solar radiation has indeed a non-negligible role in the  
59 Arctic region, which is already threatened by a two-fold temperature increase compared to the mid-  
60 latitude areas, the so-called “Arctic Amplification” (Bond et al., 2013; Cohen et al., 2014; Serreze and  
61 Barry, 2011). BC has an atmospheric lifetime of about seven days and has been directly targeted in  
62 important international mitigation agreements (AMAP, 2015). Theoretical and experimental results  
63 showed that the cryosphere is affected both by the BC-induced warming of the atmosphere and by direct  
64 and indirect BC effects on the snow once deposited over it (Flanner, 2013),



65 Atmospheric BC measurements in the Arctic regions are still rare, despite an extraordinary effort  
 66 done by the international scientific community to evaluate the sources, transport paths, concentration, and  
 67 climate impact (Eleftheriadis et al., 2009; Pedersen et al., 2015; Ferrero et al., 2016; Ruppel et al., 2017;  
 68 Osmont et al., 2018; Zanatta et al., 2018; Laj et al., 2020). BC mass concentrations can be measured  
 69 directly by using incandescent or thermal techniques and indirectly, by absorption measurements using an  
 70 appropriate mass absorption cross-section (Petzold, 2013). Various terms such as refractory black carbon  
 71 (rBC) for incandescent measurements, elemental carbon (EC) using thermal techniques, or equivalent  
 72 black carbon (eBC) based on optical technique are used. Forsström et al. (2009) reported measurements  
 73 performed in Arctic snow in the past and new measurements of EC in snow surface using filters and a  
 74 thermo-optical method. The geographical and seasonal eBC variability was investigated in the Arctic  
 75 region by Doherty et al. (2010). Other BC measurement in snow samples from the Arctic region can be  
 76 found in Aamaas et al. (2011), Forsström et al. (2013), Pedersen et al. (2015), Gogoi et al. (2016), Khan  
 77 et al. (2017) and Mori et al. (2019). Intercomparison of different techniques agree within a factor of 2  
 78 uncertainty at Alert (Sharma et al., 2017), Ny-Ålesund, and Barrow (Sinha et al., 2017).

79 A complex combination of processes are involved in the BC particles transfer from the  
 80 atmosphere to the surface snow. Via a modelling approach, Liu et al. (2011) found that approximately  
 81 50% of BC's total burden in the Arctic atmosphere is removed through wet deposition-related processes.  
 82 Yasunari et al. (2013) estimated the intensity of BC dry deposition on the Himalayan glaciers; they found  
 83 that the surface roughness and the surface wind speed are critical parameters in order to retrieve realistic  
 84 results. Emerson et al. (2018) empirically evaluated the in situ rBC deposition velocities over a grassland  
 85 ( $0.3 \pm 0.2 \text{ mm s}^{-1}$ ), suggesting eddy covariance as the main deposition driver. In a recent study, Jacobi et  
 86 al. (2019) confirmed the previous estimates suggesting that approximately 60% of the BC particles are  
 87 deposited on the surface snow via wet deposition in spring in the Svalbard Arctic area. Models are still  
 88 not fully able to describe the actual deposition and transport processes in Svalbard, resulting in  
 89 underestimating the BC concentration in the snowpack (Eckhardt, S. et al 2015, Stohl, A. et al. 2013).  
 90 Although wet deposition is suggested to be the main driver of BC concentration in the snow, little is  
 91 known about other environmental processes potentially affecting the BC particles concentration once  
 92 deposited, i.e. physical post-depositional processes.

93 In this study we present two unique experiments performed in a clean area close to the town of  
 94 Ny-Ålesund (Svalbard) at the Grubebadet Aerosol Laboratory (78.91734 N, 11.89535 E, 40 m a.s.l.),  
 95 during spring 2014 and 2015. Daily and hourly time resolution samplings were performed on the snow  
 96 surface to investigate which atmospheric variables could directly or indirectly modify the BC mass  
 97 concentration in the surface snow once deposited. The daily sampling lasted for approximately 85 days to  
 98 assess the seasonal variability covering the transition from a cold period (April) to the melting period in



late May. The hourly time resolution experiment was performed to investigate potential processes affecting the BC concentration over the diurnal cycle.

## 2. Experimental Methods

### 2.1 Study Area

Both experiments were conducted in the proximity of the Ny-Ålesund research station (78.5526 N, 11.5519 E, 25 m a.s.l.), located on the Spitzbergen island in Svalbard archipelago. Along the west coast, Svalbard is characterized by a maritime climate with an annual average temperature of -3.9°C in Ny-Ålesund (between 1994 and 2017) (Maturilli et al., 2019). On average, the snowpack starts building up in September and melts away at the end of May (Førland et al. 2011). Ny-Ålesund has become one of the reference locations for conducting Arctic climate studies focusing on atmospheric composition and physics. Long-term monitoring of atmospheric aerosols is performed at the Gruvebadet station (Feltracco et al., 2019; Moroni et al., 2018; Ferrero et al., 2016; Bazzano et al., 2015; Moroni et al., 2015; Zangrando et al., 2013; Scalabrin et al., 2012), and at the Zeppelin observatory (475 m a.s.l.) (Eleftheriadis et al., 2009; Tunved et al., 2013; Lupi et al., 2016, and reference therein).

### 2.2 Snow Sampling

There are no standardized methods for sampling, filtering and analytical protocols for detecting atmospheric carbon deposited in snow, even if a few protocols have been developed (Ingersoll et al., 2009; Gallet et al., 2018; Meinander et al., 2020). In the present work two different sampling strategies were adopted regarding the thickness of the sampled layer and the temporal sampling frequency.

Snow samples were collected during two field campaigns: The first campaign was carried out in Spring 2014, from April 1<sup>st</sup> to June 24<sup>th</sup> for a total of 85 days, it consists of daily sampling and it is referred hereafter as the “85-days experiment”. The second campaign was conducted in Spring 2015 from April 28<sup>th</sup> to May 1<sup>st</sup>. During these three days, measurements were collected with hourly sampling. This second campaign is hereafter referred as the “3-days experiment”. Snow samples were collected about 1 km North-West of Ny-Ålesund (Figure 1). The area is a dedicated clean site for aerosols and snow sampling, with no fuel engine traffic. The wind at the site is usually blowing from east to west, and rarely from North to South, minimizing the emission of the town reaching the sampling area. The main wind pattern during the experiment is presented in Figures 1 and 2. The samples for both experiments were kept frozen until the lab analyses. The samples were collected using neck nylon gloves to avoid any contamination.

The two experiments aim to capture the rBC mass concentration on a daily basis in the surface snow (upper 10 cm) during the seasonal change and on an hourly basis on a thinner surface snow layer



133 (upper 3 cm) during a daily cycle. Although wet and dry deposition are the main sources of BC in the  
134 Arctic snow, the aims of our experiments were to evaluate if other atmospheric parameters could  
135 contribute to the snow surface rBC mass concentration variability.

136 In the 85-days experiment, the first 10 cm of surface snow were collected on a daily basis  
137 (approximately at 11.00 am, GMT+2) in the same area, using a 5 cm diameter and 10 cm long Teflon  
138 tube. The samples were collected following a straight line leaving about 15 cm between the sampling  
139 points to minimize the spatial variability. The collected snow was homogenized in a pre-cleaned plastic  
140 bag and then, without melting, 50 mL was transferred into vial (Falcon™ 50mL Conical Centrifuge  
141 Tubes) for BC, coarse mode particles number concentration and electrical conductivity analyses. The 85-  
142 days experiment was designed with the aim to investigate the BC presence in the upper snow layer, where  
143 most of the snow-radiation interaction takes place and where BC particles' presence can decrease the  
144 snow albedo (Doherty et al., 2010). Moreover, this sampling strategy allowed to evaluate the variation of  
145 BC on a seasonal basis and to capture the impacts of wind, precipitation or melting.

146 During the 3-days experiment, the first 3 cm of surface snow were collected on an hourly basis in  
147 pre-cleaned vials in a delimited area of 2 x 2 m using the same sampling tools as above (Spolaor et al.,  
148 2019). In this case the samples were collected following a straight line leaving about 5 cm between the  
149 sampling points. The aim of the 3-days experiment was to investigate the potential daily cycle of surface  
150 BC concentration; therefore, we foresaw that small variations could derive from the impact of the daily  
151 variation of solar zenith angle and subsequent induced snow metamorphism at the surface of the  
152 snowpack, often at cm scale. To avoid dilution of the signal, we reduced the vertical sampling thickness  
153 to 3 cm to enhance our chances of observing variation in the rBC mass concentration if such variation  
154 exists.

155 The temperature at the surface of the snowpack (at 7 cm for 85-days and at 3 cm for 3-days  
156 experiment) was always measured. The daily/hourly snow accumulation was determined by measuring  
157 the emerging part of 4 poles placed around the sampling area. The average standard deviation calculated  
158 from the four poles provides us a reasonable estimate of the variability in snow accumulation/depletion  
159 within the sampling area. The standard deviation obtained ranges from 2 to 4 cm for the entire periods,  
160 indicating a limited spatial variability.

161

## 162 **2.3 Atmospheric Optical Measurements**

### 163 **2.3.1 Aethalometer (AE-31)**

164 In this study, the equivalent BC (eBC) concentration in the Boundary Layer (around 3 m a.s.l.)  
165 was measured by an AE-31 aethalometer (Gundel et al., 1983), during the 3-day campaign. The device is  
166 equipped with 7-wavelengths (370, 470, 520, 590, 660, 880, 950 nm). It determines the attenuation



coefficient by using the light attenuation ratio through a sensing spot and a referenced clean spot, both on a quartz fiber filter substrate. The sampling and reference spots surface areas are  $0.5 \text{ cm}^2$ , while the volumetric flow rate is  $4 \text{ l min}^{-1}$ . The flow rate was calibrated with a TetraCal (BGI Instruments) volumetric airflow before and after the field campaign. A 5 minutes temporal resolution was used for data acquisition. However, due to the low background concentration in the Arctic, the signal/noise ratio is high, so that data were hourly averaged. The data presented in this study were processed according to Segura et al. (2014) methodology. For this purpose the multiple scattering and filter loading effect (Weingartner et al., 2003) was corrected with new values of mass absorption cross section (MAC) and multiple scattering factor ( $C=3.1$ ), reported by Zanatta et al. (2018). The MAC value was derived using observations and observationally constrained Mie calculations in spring at the Zeppelin Arctic station (Svalbard,  $78^\circ\text{N}$ ). Zanatta et al. (2018) estimated the MAC at  $550 \text{ nm}$  ( $9.8 \text{ m}^2 \text{ g}^{-1}$ ) and at  $880 \text{ nm}$  ( $6.95 \text{ m}^2 \text{ g}^{-1}$ ), which we used to estimate MAC at  $520 \text{ nm}$  ( $10.2 \text{ m}^2 \text{ g}^{-1}$ ).

179

### 2.3.2 Particle Soot Absorption Photometer (PSAP)

During the 85-days sampling period the aerosol absorption coefficient was also measured by means of a 3-wavelengths PSAP (this instrument was not available during the 3-days experiment period). It measures the variation of light transmission through a filter where particles are continuously deposited with constant airflow. A second filter identical to the first one remains clean and is used as a reference to take into account possible variations of the light source, i.e. a 3-color LED (blue, green and red with wavelength centred around  $470$ ,  $530$  and  $670 \text{ nm}$ , respectively). The correction developed by Bond et al. (1999) was applied to consider the filter loading effect. The complete eBC mass concentration time series for the 85-days experiment was retrieved using the Aethalometer (first period) and the PSAP (second period), with an overlapping period with simultaneous measurements of 5 days. For the retrieved eBC mass concentration from the two instruments to be equal during the overlapping period, the PSAP eBC was calculated dividing the absorption measurements (at  $530 \text{ nm}$ ) with a MAC equal to  $7.25 \text{ m}^2 \text{ g}^{-1}$  (keeping the AE31 data as reference). Daily averages were calculated from the 1-minute data to compare with the rBC daily data obtained from the snow.

194

## 2.4 Surface Snow measurements

### 2.4.1 Coarse Mode Particles Number Concentration

The snow samples were melted at room temperature before the on-line coarse-mode particles and conductivity measurements (the water was pumped from the vials by a 12 channels peristaltic pump, ISMATECH, type ISM942). Specifically, the number concentration of coarse mode particles in the surface snow was measured with a Klotz Abakus laser sensor particle counter. This instrument optically



counts the total number of particles and measures each particle's size in a liquid constantly flowing through a laser beam cavity (LDS 23/23). The measurements size range of the instrument is from 0.8 to about 80  $\mu\text{m}$  with 32 dimensional bins (Table SI 1), not overlapping with that of the SP2. Only the 32<sup>nd</sup> bin has a dimensional range above 15.5  $\mu\text{m}$ , i.e. of 80  $\mu\text{m}$ . The data were recorded by a LabView® based software obtaining a sufficient number of data points in order to have a standard deviation of the mean smaller than 5%. The particles number concentration was calculated using the constant water flow value.

207

#### 2.4.2 rBC Measurement – SP2

The rBC mass concentration and mass size distribution were measured following the methods described in Lim et al. (2014). The snow samples were melted at room temperature prior to the analyses. The vials with the melted snow were sonicated for ten minutes at room temperature. The samples were nebulized before the injection in the Apex-Q desolvation system (APEX-Q, Elemental Scientific Inc., Omaha, USA). The nebulization efficiency was evaluated daily by injecting Aquadag® solutions with different mass concentrations, ranging from 0.1 to 100  $\text{ng g}^{-1}$ , obtaining an average value of 61%, that was used to correct all the BC mass concentrations reported in this manuscript. More details on the method can be found in Lim et al. (2014) and in Wendl et al. (2014).

The SP2 data were analyzed using the IGOR based toolkit from M. Gysel (Laboratory of Atmospheric Chemistry, Paul Scherrer Institute, Switzerland). The large amount of signals derived from every single particle are elaborated achieving rBC mass and number concentrations and size distributions.

220

#### 2.5 Meteorological Parameters

Meteorological parameters, in addition to the atmospheric and snow ancillary measurements, were used in the statistical exercise to study the variability of rBC mass concentration in surface snow samples as a function of the atmospheric conditions. BC particles are deposited on the snowpack following a combination of wet and dry deposition. However, once deposited on/in the snowpack other processes can potentially induced a significant variability in the surface BC content. The wind direction and its velocity can modify the BC distribution in the upper snowpack due to snow-mobilization. The solar radiation and relative humidity may enhance snow sublimation and surface hoar formation thus modifying the relative BC concentration in the upper snow layer by removing or adding “water” mass to the snow surface.

Air temperature and relative humidity at 2 meter height have been retrieved from a meteorological station located about 800 meters north of the sampling site, using a ventilated PT-100 thermo-couple by Thies Clima and a HMT337 humicap sensor by Vaisala, respectively. Wind speed and direction at 10 meter height were obtained from a Combined Wind Sensor Classic by Thies Clima (see Maturilli et al., 2013).





At about 50 m distance, the radiation measurements for the Baseline Surface Radiation Network (BSRN) provide among others the downward solar radiation detected by a Kipp&Zonen CMP22 pyranometer (Maturilli et al., 2015). Both meteorological and surface radiation measurements are available in a 1-minute time resolution via the PANGAEA data repository (Maturilli et al., 2020). The daily/hourly mean values of the meteorological parameters were used in the statistical analyses of the 85-days/3-days experiment and in Figure 2 and Figure 3 (the physico-chemical parameters from the snow samples are punctual values).

## 2.6 Parameters consider in the statistical analysis

The snow pack evolution is primarily driven by meteorological parameters, which are responsible for adding/removing mass to the annual snow pack. Wind can affect the snow pack evolution in several ways: 1) by snow redistribution, 2) favouring the ablation\sublimation, and 3) lifting particles from nearby sources and areas. Surface snow and air temperatures are two fundamental parameters required to fully understand the varying conditions of the snow pack. In our study, the temperature variables are proxies for the melting episodes and for the presence of liquid water potentially affecting the concentration of impurities. The incoming solar radiation is not expected to be directly linked to the surface mass concentration of rBC, however the surface process could affect it indirectly by favouring sublimation (water mass removal), as well as hoar formation (water mass addition) during the colder parts of the day (night/early morning). The relative humidity gives an idea of the amount of water present in the atmosphere and the high RH might favour the deposition of BC suspended by the formation of water droplets through the cloud condensation nuclei, this is especially significant for the selected sampling location, nearby to the shore. The last meteorological parameter considered is the precipitation amount. This is important to understand the wet deposition processes able to transfer BC particles from the atmosphere to the snow surface.

The additional selected parameters are 1) the atmospheric eBC mass concentration, an interesting parameter to investigate the potential transfer function of BC particles from the atmosphere into the snow surface, 2) the coarse mode particles (dust) that could have a similar transport pathways to the black carbon and gives an idea of the amount of total impurities deposition and 3) the total water conductivity, an indirect measurement of the salinity content of the snow. Considering the location of the sampling site (<1km from the coast line), the contribution of the ocean emissions to the snow pack chemical composition is significant. We considered the total conductivity as an indication of sea spray deposition, and to investigate common deposition pattern and/or similarities to the behaviour of BC (although BC is not emitted from ocean surface). The conductivity was also considered to determine if there was a large





268 sea-spray aerosol event, which could bring a lot of salt, potentially affecting the SP2 measurements (see  
269 supplementary material).

270

## 271 **2.7 Statistical Analysis**

272 Multiple linear regression was carried out to evaluate the relationship between the observed  
273 surface snow rBC mass concentration and the selected set of covariates consisting of the meteorological  
274 and snow physico-chemical parameters that could have a direct effect controlling snowpack dynamics as  
275 well on the BC concentration as discussed in Section 2.6. All the atmospheric parameters described in the  
276 previous section (wind, snow and air temperature, incoming solar radiation, relative humidity and snow  
277 precipitation amount) were initially considered as covariates to be included in the multiple linear  
278 regression. However, wind speed and direction, as well as the atmospheric stability, expressed as vertical  
279 wind speed, were removed because preliminary statistical analyses indicate that none of them is  
280 associated with the observed variations in snow rBC mass concentrations. This does not mean that such  
281 parameters do not play a role in controlling the BC concentration, but that no statistically significant  
282 associations were found with the data collected in our study and thus these parameters no longer  
283 considered in the statistical analyses discussed below.

284 Hence, the fitted multiple regression models are designed to describe the variation in snow rBC  
285 concentrations as a function of atmospheric eBC concentration, surface snow coarse mode particles  
286 number concentration, snow temperature (7 cm depth for 85-days experiment and 2 cm depth for the 3-  
287 days experiment), snow precipitation, solar radiation and conductivity. Since the covariates considered in  
288 the two experiments have quite different unit scales, the covariates have been standardized before fitting  
289 the regression models. The standardization simplifies the comparison among the estimated effects of the  
290 different covariates and between the two experiments, in this way facilitating the interpretation of the  
291 results and their discussion. Further details about the statistical analyses are given in the Supplementary  
292 material.

293 It is important to note that the eBC and the rBC mass concentrations are not the same physical  
294 quantities: the former is obtained from an absorption measurement assuming a constant MAC, whereas  
295 the second is obtained via a laser-induced-incandescence method with an SP2 empirically calibrated with  
296 a reference material (Petzold et al., 2013).

297

## 298 **3. Results and Discussions**

### 299 **3.1 Seasonal BC variability in surface snow**

#### 300 **3.1.1 Atmospheric eBC concentrations**



During the experimental period, the atmospheric eBC concentration shows a noticeable variability ranging from  $80 \text{ ng m}^{-3}$  to  $< 5 \text{ ng m}^{-3}$  (Figure 2). The highest concentrations were measured at the beginning of the campaign, especially from April 15 to 27, followed by a general decreasing trend characterized by the presence of several concentration peaks (on May 8, 17 and 24) potentially due to Eurasian fires, as already suggested from Feltracco et al., 2020 (Figure S1). The ammonia daily concentration time series (the only available biomass burning tracer for that period in the area) measured at the Zeppelin station is plotted together with the Gruvebadet atmospheric BC measurements in Figure S3. Biomass burning is a significant source of atmospheric ammonia (Andreae and Merlet, 2001), often affecting the Arctic region (Moroni et al. 2020). As shown in Figure S3, both time series have a similar behaviour at the very beginning of the campaign, from April 3 to 8 and during the period between May 7 and 21. This suggests that the BC detected in the atmosphere could be originated from biomass burning episodes during these two time periods.

313

### 3.1.2 Surface Snow and Atmospheric Conditions

During the 85-days sampling period, wind was characterized by the following median values (25<sup>th</sup> and 75<sup>th</sup> percentiles) for direction and speed:  $205^\circ$  ( $152^\circ$ ,  $257^\circ$ ) and  $2.7$  ( $1.9$ ,  $3.7$ )  $\text{m s}^{-1}$ , respectively, therefore mostly coming from South-West (Figure 2). Daily air temperature at 3 m increased during the campaign from  $-15^\circ\text{C}$  to about  $+5^\circ\text{C}$  (Figure 2) following the seasonal variation of incoming solar energy: from  $100$  to  $300 \text{ W m}^{-2}$  with an average of  $185 \pm 75 \text{ W m}^{-2}$  (Figure 2, orange line). The snow precipitation episodes are presented as daily-accumulated values (Figure 2, blue bars) ranging from zero to 12 cm. The atmospheric eBC mass concentration, derived from the PSAP absorption coefficient, shows a decreasing trend during the campaign, ranging from 2 to  $80 \text{ ng m}^{-3}$  with an average of  $34 \pm 23 \text{ ng m}^{-3}$ .

Over the 85 days experiment, the snow rBC mass concentration varies from  $0.2$  to  $6 \text{ ng g}^{-1}$  (Figure 2), with an average of  $1.4 \pm 1.3 \text{ ng g}^{-1}$ , in agreement with results available in the literature (Mori et al., 2019; Jacobi et al., 2019; Aamaas et al., 2011). An increasing trend can be observed for the rBC mass concentration in the surface snow across the sampling period. The median of the rBC mass equivalent diameter in the snow is  $313 \pm 35 \text{ nm}$  (Figure 2), similar to what obtained in other studies (e.g. Schwarz et al., 2013). The rBC mass equivalent diameter show high variability, ranging from 200 to 500 nm. However, since the rBC concentrations were low, the evaluation of the particles geometric mean diameter for the biggest sizes, above 300 to 400 nm, has only to be considered as qualitative information given the high noise in the size distributions.

The number concentration of coarse mode particles (Figure 2, blue line) shows a constant concentration in the first half of the campaign, until May 11, whereas increases in the second half, especially after the 1<sup>st</sup>



of June, in concomitance with the onset of the snow melting period; the average number concentration is  $4914 \pm 4109 \text{ \# ml}^{-1}$ . The conductivity (Figure 2, green line) shows as well an increasing trend at the end of the sampling campaign when snow is melting, with an overall average value of  $30 \pm 8 \text{ \mu S}$ . The spatial variability of BC, calculated in the same manner as proposed by Spolaor et al. (2019) for other species, was obtained from 6 surface snow samples collected in the four corners of the sampling area and two in the centre right before the beginning of the experiment. The following rBC mass concentrations were obtained: a)  $3.95 \text{ ng g}^{-1}$ ; b)  $4.92 \text{ ng g}^{-1}$  c)  $4.20 \text{ ng g}^{-1}$  d)  $3.10 \text{ ng g}^{-1}$  e)  $3.82 \text{ ng g}^{-1}$  f)  $3.58 \text{ ng g}^{-1}$ , resulting in a BC spatial variability of 16% in the surface snow in the considered sampling area.

342

### 3.1.3 Statistical Results

The fitted multiple linear regression model for the 85-days experiment data explains 69% of the total variance of snow rBC mass concentration ( $R^2 = 0.69$ ). Statistically significant associations are found among the snow rBC mass concentration and the coarse-mode particles number concentration ( $p < 0.001$ ), the amount of snow precipitations ( $p = 0.03$ ) and the snow temperature ( $p < 0.001$ ). The statistical associations of rBC mass concentration with the other covariates considered in the model were non-significant (see Table 1 reporting the standardized estimated coefficients and the corresponding p-values). Figure 4 displays both the 95% confidence intervals for the 85-days campaign and the 3-days experiment in a way to allow a visual comparison of the estimated statistical associations between the snow rBC mass concentration and the considered parameters.

In order to interpret the statistical results, the description of the 85-days campaign is split into two periods identified as the transition from the “cold” to the “melting” state. The first period occurred before the end of May: the rBC mass concentration often increases with snowfall episodes (April 9/10/11 and 17; May 17, 22 and 27/28; June 1) as suggested by previous studies, with exceptions for April 24 and May 7. Over the sampling period, a weakly statistically significant positive association ( $p = 0.03$ ) was found between snow rBC mass concentration in surface snow and the daily amount of snow precipitation. BC wet deposition processes are estimated to remove 50% - 60% of the total atmospheric BC burden in the Arctic (Liu et al., 2011; Jacobi et al., 2019). In our study, the wet deposition impacts could be partially masked due to the sampling frequency and the wind snow. In Kongsfjord, a strong wind is often present when precipitation events occurred (Figure 2). Consequently, the freshly deposited snow is frequently removed from the surface before being able to sample it. Usually, the sampled snow at the surface is not made of the freshly precipitating but by redistributed surface snow. Interestingly, our observations show that, on a daily scale, the precipitation episodes are not clearly related to a decrease in the atmospheric eBC mass



366 concentration (Figure 2). A possible explanation is that the precipitation amounts were small so that the  
367 precipitation events did not alter significantly the atmospheric BC reservoir.

368 In the second period, from the beginning of June, the atmospheric temperature increases, causing the  
369 snow-melting season's onset. At the beginning of June, the snow rBC mass concentration increases up to  
370 approximately  $5 \text{ ng g}^{-1}$ , and a simultaneous increase was detected in the coarse mode particles number  
371 concentration (peaks between June 4 and 7). As suggested in previous studies, the surface melting process  
372 could explain the observed increase in BC and dust particles concentrations. However, we also have to  
373 consider that both BC and dust can be dry deposited. Dry deposition is the main depositional process for  
374 the coarse mode particles. Recently it has been suggested to have a significant contribution to the BC  
375 surface content (up to 50-60%; Liu et al., 2011; Jacobi et al., 2019). Very few field validation data exist  
376 for estimating the amount of dry deposited at the snow surface, and this process is often used as an  
377 ancillary information since most models underestimate the BC in the Arctic snowpack compared to field  
378 measurements.

379 Our data support the hypothesis related to local sources' activation in enhancing the dry deposition  
380 impacts in an old mining town as Ny-Alesund. Especially during poor snow cover conditions, as during  
381 the snow-melting season, dust particles as residuals of carbon extraction mining activities are available  
382 for wind lift/suspension. The possible effect of local sources' activation is further supported by a recent  
383 analysis of the Broggerbreen glacier and Ny-Alesund annual snow pack. This analysis shows the presence  
384 of Retene (an organic compound frequently used to track the presence of coal), most likely due to local  
385 sources (Vecchiato et al., 2018).

386 The simultaneous increase of rBC mass and coarse mode particle number concentrations during the  
387 second part of the experiment (e.g. visible between June 3 and 7-8) could be explained via similar post-  
388 depositional processes: snow melting and sublimation. The episodes of snow surface melting can  
389 significantly affect the snow particulate content and we hypothesize that the hydrophobicity of pure BC  
390 particles, and of several species in the coarse mode particles, might affect its physical location in the  
391 snowpack (in the literature, the response of the BC particles is still debated): the hydrophobicity of the  
392 particles can cause the surface concentration to increase while losing water mass through percolation.  
393 This could lead into a positive feedback process: the increase of BC concentration can thus enhance snow  
394 sublimation (water evaporation) resulting in a further increase of BC concentration in surface snow, and  
395 so on.

396 In this study, the estimated statistical association between snow rBC mass concentration and the daily  
397 snow temperature is negative and strongly significant ( $p < 0.001$ ). During the 85-days experiment, we can



distinguish two events where the temperature appeared to play a role in the BC concentration. Both of them show an increase in rBC mass concentration during melting/refreezing episodes, in agreement with other studies (Aamaas et al., 2011). The first event occurred between May 5 to 12 and the second after May 20, when the proper snow melting began (Figure 2). The first event was characterized by a rapid rise of daily air temperature (from  $-6^{\circ}\text{C}$  to  $-1^{\circ}\text{C}$ ) in concomitance to a snow precipitation event, followed by a rapid temperature decrease to  $-6^{\circ}\text{C}$ . The surface snow (10 cm) mirrored this behaviour, first rising from  $-6^{\circ}\text{C}$  to  $0^{\circ}\text{C}$ , and then cooling down to  $-6^{\circ}\text{C}$ . During this warm event, the upper snow strata underwent a melting episode with surface water percolation (although limited), making the surface BC concentration to increase. The second event started approximately on May 20 and lasted until the end of the experiment (Figure 2). During this period, the atmospheric temperature increased constantly, and the snowpack started to melt consequently. Moreover, surface BC concentration increased almost continuously from May 25 to its maximum observed in June 6. Afterward, the upper snow rBC mass concentration tended to decrease following the rapid snowpack decline.

411

### 412 3.2 Diurnal variation of rBC in surface snow

#### 413 3.2.1 Surface Snow/Atmospheric Aerosol Content and Atmospheric Conditions

414 The 3-days experiment was performed at the end of April 2015, during the Arctic spring. The  
415 samples were collected on an hourly basis over 3 days achieving a high-resolution sampling frequency.  
416 The atmospheric concentration of eBC ranged from 2 to  $50\text{ ng m}^{-3}$ , decreasing during the sampling period  
417 and not showing any particular diurnal pattern (Figure 3). The mean value of the atmospheric eBC mass  
418 concentration is  $34 \pm 23\text{ ng m}^{-3}$ , similar to the average of the 85-days experiment.

419 The surface snow rBC mass concentration exhibited hourly variability showing up to 2-fold  
420 hourly increases (especially during the first day), overlapping a daily variation (Figure 3, bottom panel,  
421 smoothed dark blue line). rBC mass concentrations of approximately  $15\text{ ng g}^{-1}$  were measured in the snow  
422 samples from the beginning of the sampling to the end of the second day. Later, from the beginning of the  
423 third day until the end of experiment, rBC mass concentrations show an average concentration of about  $5\text{ ng g}^{-1}$   
424 (Figure 3). The average value over the whole sampling period is  $9.5 \pm 5.2\text{ ng g}^{-1}$  (approximately 6  
425 times higher than during the 85-days experiment). The rBC mass size distribution was characterized by a  
426 median value of the geometric means of about  $230 \pm 32\text{ nm}$ , significantly lower than that which was  
427 measured during the 85-days, and still in agreement with previous studies (Sinha et al., 2018; Bond et al.,  
428 2013). The concentrations of EC and OC measured in parallel snow samples (not of the same volume) are  
429 reported and described in Figure S4; the interpretation of the differences between the rBC and the EC  
430 measurements in snow samples was beyond this manuscript's objectives.



431 The number concentration of coarse mode particles remains stable in the first half of the  
432 experiment, until the end of April, and shows an average value over the three days of  $26642 \pm 9261 \text{ \# ml}^{-1}$   
433 <sup>3</sup>. The water conductivity shows a similar behaviour, and it is characterized by an average of  $39 \pm 9 \text{ \mu S}$   
434 (30% higher than during the 85-days experiment).

435 All the measured snow impurities time series show two common features: first, a decrease in the  
436 absolute values detected between 4 and 8 a.m. of April 30, despite the absence of precipitations and of  
437 any particular meteorological episode (Figure 3); second, the impact of the snow precipitation event from  
438 approximately 4 p.m. to midnight of the April 30, where the concentrations of aerosols in the snow  
439 slightly increased at the very beginning whereas decreasing at the end of the event. Only the BC core  
440 diameter remained above the average when the other aerosol snow content decreased (up to  
441 approximately 400 nm of mass equivalent diameter), consequently returning to the average value. The  
442 spatial variability of BC, calculated as proposed by Spolaor et al. (2019) for other species, was obtained  
443 by the analysis of 5 surface snow samples, collected in the four corners of the sampling area and one in  
444 the centre obtaining the following concentrations: a)  $10.17 \text{ ngg}^{-1}$ , b)  $10.64 \text{ ngg}^{-1}$ , c)  $7.04 \text{ ngg}^{-1}$ , d)  $11.98$   
445  $\text{ngg}^{-1}$ , and e)  $11.91 \text{ ngg}^{-1}$ , thus resulting in a spatial variability of 19%. Clear sky conditions were  
446 observed for the duration of the sampling period except for the snowfall occurred at the end of the third  
447 day.

448

### 449 3.2.2 Statistical Results

450 The multiple linear regression model for the 3-days experiment explains the 83% of the total snow rBC  
451 mass concentration variance, a percentage higher than the 85-days experiment, likely due to the more  
452 stable atmospheric conditions and the greater interaction with the atmosphere of the upper 3 cm compared  
453 to the 10 cm used for the seasonal experiment. The fitted multiple linear regression model indicates a  
454 statistically significant association between the rBC mass concentration in the snow and the conductivity  
455 ( $p < 0.001$ ), the number concentration of coarse-mode particles ( $p = 0.003$ ), the snow precipitation  
456 amount ( $p < 0.001$ ), the incoming solar radiation ( $p = 0.009$ ) and the snow temperature ( $p = 0.01$ ). The  
457 standardized estimated coefficients are reported in Table 1, displayed along with 90% and 95%  
458 confidence intervals in Figure 4.

459 The association between the coarse-mode particles number concentration and the snow rBC mass  
460 concentration is positive and strongly significant ( $p < 0.001$ ), similarly to what observed for the 85-days  
461 experiment, confirming the similar behaviour of these types of particles.

462 A negative association is found between the rBC mass concentration in the snow and the  
463 incoming solar radiation ( $p = 0.009$ ), and a weaker negative association with the snow temperature ( $p =$   
464  $0.01$ ). The latter is strongly dependent on the solar radiation. This relation suggests that the rBC mass



concentration in surface snow might undergoes to a diurnal variation: low mass concentrations when the solar radiation is high and vice versa. The BC particles are known to be non-volatile and not photochemically active, therefore the decrease in their concentration observed when the solar radiation is higher could not be explained as a re-emission process from the snowpack into the atmosphere as observed for other aerosol species (Spolaor et al., 2018; Spolaor et al., 2019). The results show that the highest rBC mass concentration levels are detected in the samples collected in the late afternoon. The late night/early morning concentration decrease is connected with the surface hoar formation (clear sky condition is essential for the hoar formation) able to dilute the surface snow BC concentration. Specifically, the lowest rBC mass concentration value is found between 5 a.m. and 12 a.m. and in the same time interval the solar radiation increases from 100 to 400 W m<sup>-2</sup>, followed by a delay of the air and the snow temperatures increase. In these time frames, the temperature offset between the air and the surface snow is the highest, up to 4°C, with the surface snow being the coldest between the two. Condensation of water vapour on the top of the snow crystals is likely adding “water” mass (without BC particles) in the collected samples and diluting the original rBC mass concentration. This process could also explain the positive statistical association between snow rBC mass concentration and conductivity ( $p < 0.001$ , Table 1 and Figure 4) mostly influenced by the presence of sea salt in the snow samples. In fact, considering the proximity of the sampling site to the coastline ( $< 1$  km), the marine spray deposition mainly controls the total conductivity. The slight increase in conductivity, as well as in the sodium concentration (Spolaor et al., 2019), determined during the night time could be associated to the formation of ice nuclei from the sea spray aerosol particles present in the atmosphere surrounding snowpack. The lower night temperature could exponentially increase the ice nuclei formation, favouring the deposition of suspended sea spray aerosol (DeMott et al., 2016).

The snow precipitation amount is negatively associated with the rBC mass concentration in the snow ( $p < 0.001$ ). As previously remarked, the aerosol scavenging intensity is not measurable with snow sampling strategies based on the sampling of a constant snow thickness from the surface (3 cm in this case). We tentatively explain the negative relation observed in this study with the high frequency sampling, being able to follow the evolution of the BC particles scavenged during a snow episode (from 3 to 12 p.m. of the 30<sup>th</sup> April 2015). The beginning of the precipitation episodes appeared to remove the highest amount of BC particles, leaving the atmosphere cleaner as reflected by the lower BC mass concentration revealed in subsequent samples. The snow collected at 18:00 of April 30 showed a higher amount of rBC as well as the highest coarse mode particles number concentration and conductivity. In the next few hours, from 9 to 12 p.m., the snow precipitations were depleted in terms of aerosol content and rBC mass concentration.





From the 3-days experiment, it appeared that the physical processes affecting the surface of the snowpack, like surface hoar formation and sublimation, play an important role. Therefore, the physical characteristics of the snow layers in which BC is embedded should be more studied in order to better characterize the daily variations of BC and its impact on the albedo. The 3 days experiment took place under clear sky conditions (most of the time) and Arctic like atmospheric circulation (Figure S2): this is crucial for investigating the variations observed, highlighting the impacts of the parameters following a diurnal cycle (ISR, snow metamorphism). This daily variability showed that the highest concentration of rBC is found during mid-day/afternoon, when the incoming solar radiation is high. In conclusion, the combination of snow metamorphism, which normally occur during a daily cycle, associated to the observed variability of rBC surface mass concentration could slightly modify the snow albedo during a day cycle. Although this effect might have a minor impact, more detailed studies including snow density and optical snow grain radius measurements should be pursued at centimetre vertical resolution in order to correctly estimate the radiative impact of the daily rBC variations, and confirm the findings from the proposed experiment.

512

#### 513 **4. Conclusions and Future Perspectives**

The seasonal and daily experiments (85- and 3-days long, respectively) suggest that the rBC concentration in the upper snow layer is not only due to a cumulative process such as when evaluating the entire annual snow pack but, rather by a more complex process involving atmospheric, meteorological and snowpack conditions. Our results based on a multiple linear regression models suggest that the amount of BC in the surface snow is decoupled from the BC atmospheric load. This finding suggests that, despite the potentially high atmospheric BC concentrations (as in the case of long-range transport of biomass burning plumes), the surface snow BC mass concentration can potentially remain unaffected. In both experiments the coarse-mode particles are positively associated to the snow BC mass concentration, suggesting that the BC and dust deposition undergo similar deposition and post-depositional processes in the upper snowpack. Specifically, before the beginning of the melting season, the wet deposition episodes appeared to have major impacts, whereas the activation of common local sources favour the wind resuspension from uncovered areas enhancing the intensity of dry deposition processes, triggering an accelerated snow melting positive feedback.

Our results also suggest that in order to explain the observed BC mass concentration variability during seasonal and diurnal time ranges other processes than wet and dry depositions should be considered. Post-depositional processes, as snow sublimation and melting, can remarkably affect the rBC mass concentration. Sublimation and hoar formation are affecting the BC content in the uppermost thin layer by adding/removing water mass, thus explaining the observed BC diurnal cycle (3-days hourly



sampling experiment). On the other hand, the surface melting episodes enrich the BC content in the surface layer not because of enhanced deposition but mainly because of water mass loss. In particular, the snow mass loss is stronger during the snow-melting season, where an increase in the rBC concentration could significantly alter the snow albedo and further enhance the radiative absorption, hence promoting a positive feedback. We believe our results to be representative at least of the Arctic coastal areas, characterized by similar processes and seasonality.

The remarkable diurnal and daily variability, as well as the complex interdependent mechanisms affecting the rBC mass concentration in the Arctic surface snow, makes the results of albedo-based radiative impact model of the active layer a potential source of erroneous conclusions: the impacts of long distance biomass burning episodes might be overestimated, whereas the impact of local sources and dry deposited impurities during the melting season underestimated. Further empirical studies are therefore necessary in order to improve our understanding of the involved physical mechanisms and to better constrain modelling studies.

#### Acknowledgements

This work was part of the PhD (in “Science and Management of Climate Change”) of Michele Bertò at the Ca’ Foscari University of Venice that was partly funded with the Early Human Impact ERC project. Thanks to Giuseppe Pellegrino for helping collecting the samples. Thanks to Jacopo Gabrieli and the technicians of the Ca’ Foscari University of Venice for the precious help in building up the coarse mode particles and conductivity measurement apparatus. We acknowledge the use of data and imagery from LANCE FIRMS operated by the NASA/GSFC/Earth Science Data and Information System (ESDIS) with funding provided by NASA/HQ. We want to thank Paolo Laj and the LGGE (Grenoble, France) for lending us the SP2 and Marco Zanatta for transferring the SP2 know-how on instrumental functioning and data analyses. Thanks to Martin Gysel-Beer, PSI, for the IGOR based SP2 Toolkit for SP2 data analyses. We thank Marion Maturilli and AWI for providing us with the meteorological data. Thanks to Giorgio Bertò for checking and correcting the language of this manuscript. This paper is an output of the AMIS project in the framework of “Project MIUR – Dipartimenti di Eccellenza 2018-2022”. This project has received funding from the European Union's Horizon 2020 research and innovation programme under grant agreement No 689443 via project iCUPE (Integrative and Comprehensive Understanding on Polar Environments).



565 **Data Availability**

566 Meteorological and surface radiation data are available at the PANGAEA database (Maturilli, 2015a;  
567 2015b; 2015c; 2016a; 2016b; 2018a; 2018b; 2018c; 2018d; 2018e). The data for precipitation amount at  
568 Ny-Ålesund can be accessed via the eKlima database of MET Norway. The BC data are available upon  
569 request.

570

571 **Author Contributions**

572 Author contributions. AS, EB, DC and MB conceived the experiments; AS, EB, DC, and LP collected the  
573 samples; MB measured the samples; KM and MMaz provided the atmospheric eBC concentrations; SC  
574 and DC provided the back-trajectories analyses; CV performed the statistical analyses with inputs from  
575 MB and AS. MB prepared the manuscript mainly with inputs from AS, J-C. G and DC (in the methods  
576 section from AS, KM, MMaz) and all co-authors contributed to the interpretation of the results as well as  
577 manuscript review and editing.

578

579 **Data repository**

580 Maturilli, Marion (2020): Basic and other measurements of radiation and continuous meteorological  
581 observations at station Ny-Ålesund (April, May 2014 and April, May, June 2015), reference list of 10  
582 datasets. Alfred Wegener Institute - Research Unit Potsdam, PANGAEA,  
583 <https://doi.pangaea.de/10.1594/PANGAEA.913988> (DOI registration in progress)

584

585

586

587

588

589

590

591

592

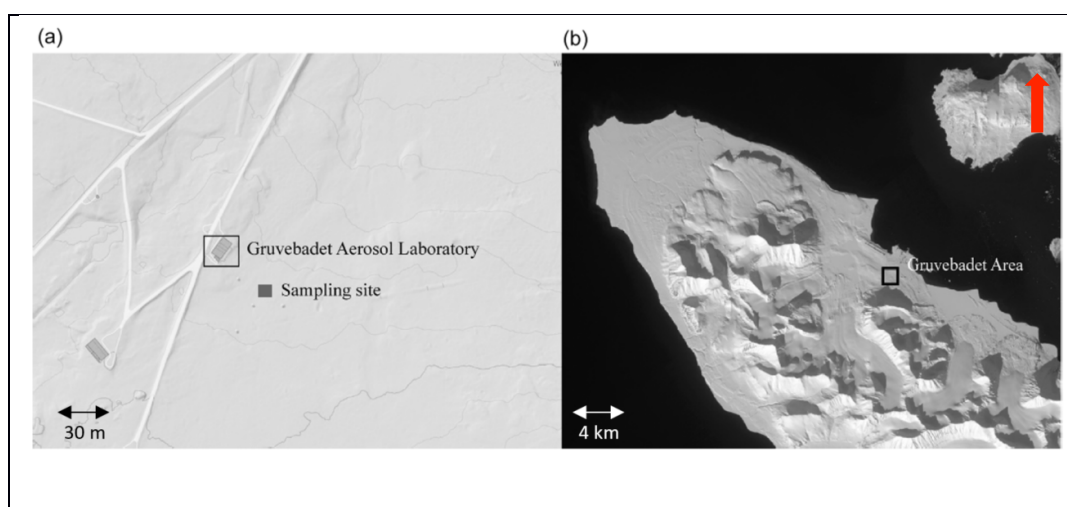
593

594



595 **FIGURES**

596 **Figure 1.** a) Experimental sampling site location (dark grey rectangle), in proximity of the Gruvebadet  
597 Aerosol Laboratory. b) Gruvebadet area (black square), close to the Ny-Ålesund research village. From:  
598 Spolaor et al., 2019 (maps from <https://toposvalbard.npolar.no/>). The red arrow points to the North.



599

600

601

602

603

604

605

606

607

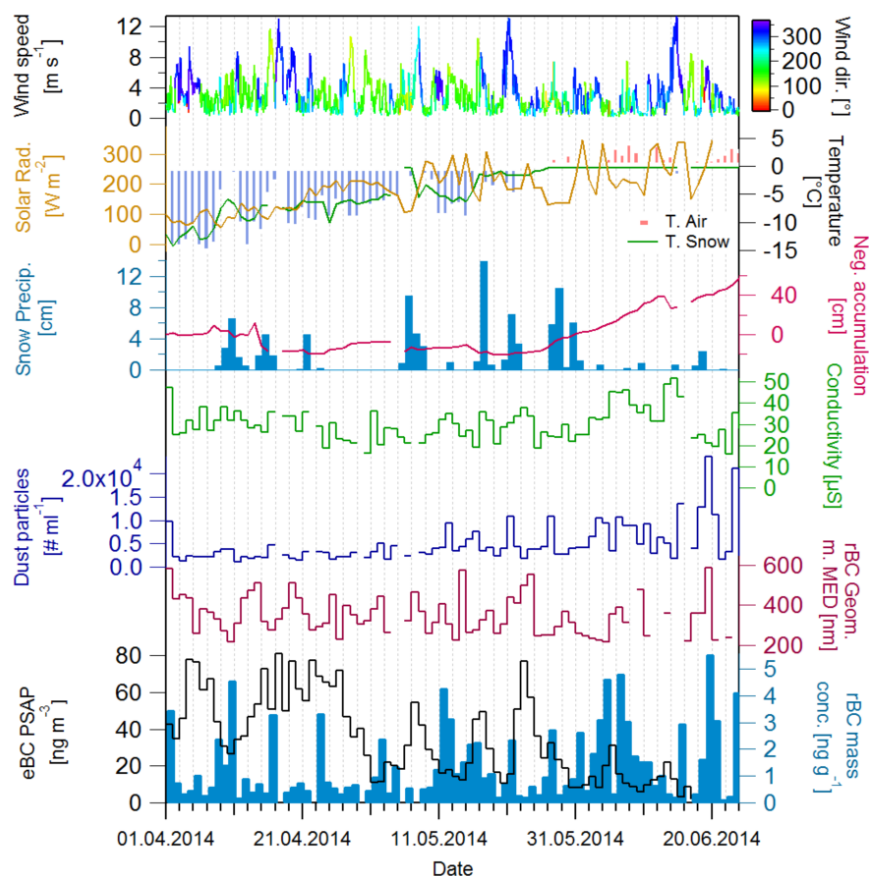
608

609

610



**Figure 2.** The 85-days experiments daily snow samples rBC mass concentration (light blue), eBC mass concentration in the atmosphere (black), geometric mean mass equivalent diameter (purple), number of coarse mode particles (blue), total conductivity (green), meteo/snow parameters used in the statistical exercise: wind speed color coded for wind direction, solar radiation (orange line), air and surface snow temperatures (blue bars and green line respectively), amount of fresh snow (“snow precipitations”, light blue bars) and the snow accumulation (“Neg. accumulation”; the values where multiplied by -1 in order to show the similar trend of the snow lost and of the air/snow temperature during the melting period at the end of the campaign).



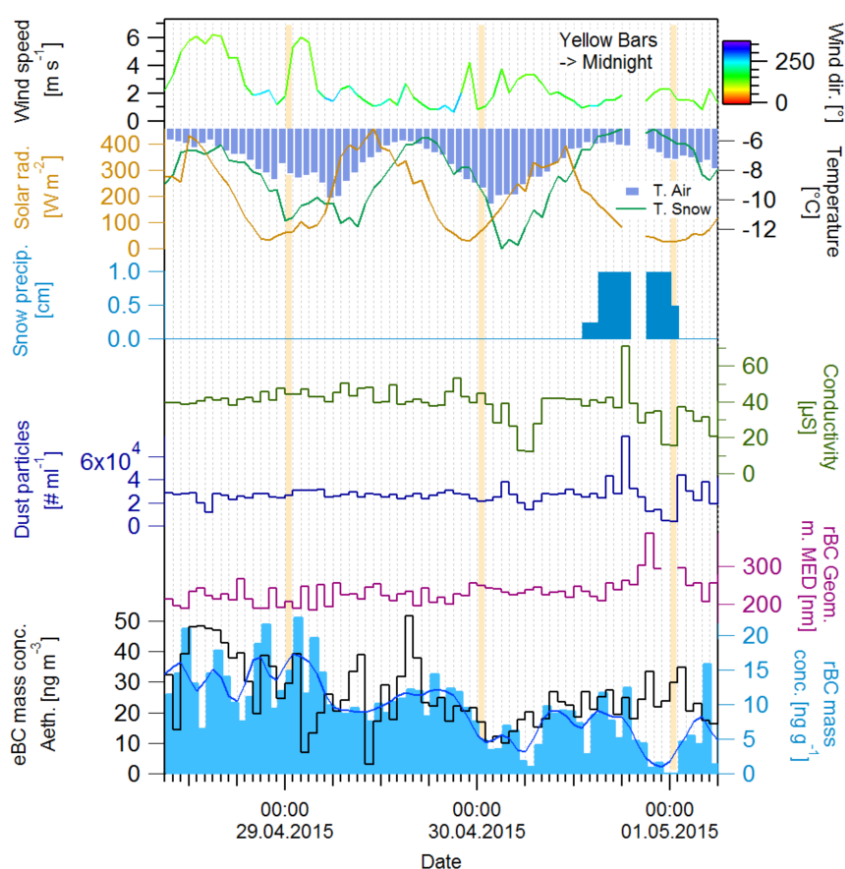
619

620

621



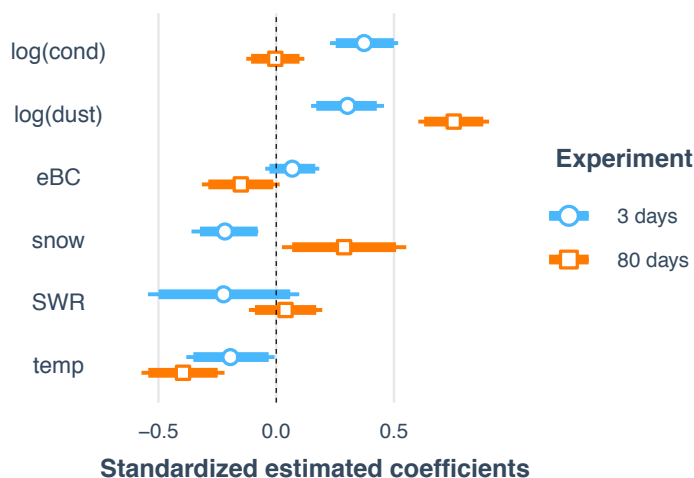
**Figure 3.** The 3-days experiments snow samples hourly rBC mass concentration and smoothed line (light blue bars), atmospheric eBC mass concentration in the atmosphere (black), geometric mean mass equivalent diameter (purple), the number concentration of coarse mode particles (blue) and the total conductivity (green), meteo/snow parameters used in the statistical exercise: wind speed color coded for wind direction, solar radiation (Orange line), Air and surface snow temperature (blue bars and green line respectively), amount of fresh snow (“snow precipitations”, light blue bars). The yellow bars are centered on the midnight hours for the three sampling days.



629  
 630  
 631  
 632



**Figure 4.** Standardized estimated coefficients of the multiple linear regression models fitted to the 3 days and 85 days experiments. The segments correspond to 95% confidence intervals about the corresponding estimates. The internal thicker segments correspond to 90% confidence intervals. Intervals that do not include the zero correspond to statistically significant covariates. If a confidence interval consists of positive values, then there is a significant positive association between the corresponding covariate and snow rBC mass concentration given the remaining covariates. Vice versa, if the confidence interval consists of negative values, then the association is negative. The abbreviations used in the plot are: “log(cond)” – logarithm of the water conductivity time series, “log(dust)” – logarithm of the coarse mode particles number concentration time series, “eBC” – equivalent black carbon atmospheric concentration, “snow” – amount of fresh snow from the precipitation episodes, “SWR” – solar radiation, “temp” – the snow temperature. The plot is produced with the R package (R Core Team, 2020) jtools (Long, 2020).



644

645

646

647

648

649

650





## 651 TABLES

652 **Table 1.** Standardized estimated coefficients and p-values for the multiple linear regression models fitted  
 653 to the 3 days and 85 days experiments data. The intercept and the trigonometric terms used to account for  
 654 the 24-hours periodicity in the 3-days experiment are not displayed.

655

Covariate	3 days	85 days
<b>log(cond)</b>	0.38 (p < 0.001)	-0.00 (p = 0.95)
<b>log(dust)</b>	0.23 (p = 0.003)	0.75 (p < 0.001)
<b>eBC</b>	0.06 (p = 0.26)	-0.15 (p = 0.07)
<b>snow</b>	-1.02 (p < 0.001)	0.29 (p = 0.03)
<b>SWR</b>	-0.43 (p = 0.009)	0.04 (p = 0.61)
<b>temp</b>	-0.23 (p = 0.01)	-0.40 (p < 0.001)
<b>R<sup>2</sup></b>	0.83	0.69

656

657

658

659

660

661

662

663

664

665

666

667

668



## 669 References

- 670 Aamaas, B., Bøggild, C. E., Stordal, F., Berntsen, T., Holmèn, K. and Strøm, J.: Elemental carbon  
 671 deposition to Svalbard snow from Norwegian settlements and long-range transport, *Tellus B Chem.*  
 672 *Phys. Meteorol.*, 63(3), 340–351, doi:10.1111/j.1600-0889.2011.00531.x, 2011.
- 673 AMAP, A. M. and A.: ARCTIC MONITORING AND ASSESSMENT PROGRAMME (AMAP): Work  
 674 Plan 2015–2017., Working Paper, Arctic Monitoring and Assessment Programme (AMAP). [online]  
 675 Available from: <https://oaarchive.arctic-council.org/handle/11374/1443> (Accessed 6 May 2020), 2015.
- 676 Andreae, M. O. and Merlet, P.: Emission of trace gases and aerosols from biomass burning, *Glob.*  
 677 *Biogeochem. Cycles*, 15(4), 955–966, doi:10.1029/2000GB001382, 2001.
- 678 Bazzano, A., Ardini, F., Becagli, S., Traversi, R., Udisti, R., Cappelletti, D. and Grotti, M.: Source  
 679 assessment of atmospheric lead measured at Ny-Ålesund, Svalbard, *Atmos. Environ.*, 113, 20–26,  
 680 doi:10.1016/j.atmosenv.2015.04.053, 2015.
- 681 Bond, T. C., Anderson, T. L. and Campbell, D.: Calibration and Intercomparison of Filter-Based  
 682 Measurements of Visible Light Absorption by Aerosols, *Aerosol Sci. Technol.*, 30(6), 582–600,  
 683 doi:10.1080/027868299304435, 1999.
- 684 Bond, T. C., Doherty, S. J., Fahey, D. W., Forster, P. M., Berntsen, T., DeAngelo, B. J., Flanner, M. G.,  
 685 Ghan, S., Kärcher, B., Koch, D., Kinne, S., Kondo, Y., Quinn, P. K., Sarofim, M. C., Schultz, M. G.,  
 686 Schulz, M., Venkataraman, C., Zhang, H., Zhang, S., Bellouin, N., Guttikunda, S. K., Hopke, P. K.,  
 687 Jacobson, M. Z., Kaiser, J. W., Klimont, Z., Lohmann, U., Schwarz, J. P., Shindell, D., Storelvmo, T.,  
 688 Warren, S. G. and Zender, C. S.: Bounding the role of black carbon in the climate system: A scientific  
 689 assessment: BLACK CARBON IN THE CLIMATE SYSTEM, *J. Geophys. Res. Atmospheres*, 118(11),  
 690 5380–5552, doi:10.1002/jgrd.50171, 2013.
- 691 Cohen, J., Screen, J. A., Furtado, J. C., Barlow, M., Whittleston, D., Coumou, D., Francis, J., Dethloff,  
 692 K., Entekhabi, D., Overland, J. and Jones, J.: Recent Arctic amplification and extreme mid-latitude  
 693 weather, *Nat. Geosci.*, 7(9), 627–637, doi:10.1038/ngeo2234, 2014.
- 694 Comiso, J. C., Parkinson, C. L., Gersten, R. and Stock, L.: Accelerated decline in the Arctic sea ice cover,  
 695 *Geophys. Res. Lett.*, 35(1), doi:10.1029/2007GL031972, 2008.
- 696 DeMott, P.J., Hill, T.C., McCluskey, C.S., Prather, K.A., Collins, D.B., Sullivan, R.C., Ruppel, M.J.,  
 697 Mason, R.H., Irish, V.E., Lee, T. and Hwang, C.Y.: Sea spray aerosol as a unique source of ice  
 698 nucleating particles. *Proceedings of the National Academy of Sciences*, 113(21), pp.5797–5803, 2016.
- 699 Doherty, S. J., S. G. Warren, T. C. Grenfell, A. D. Clarke, and R. E. Brandt. "Light-absorbing impurities  
 700 in Arctic snow." *Atmospheric Chemistry and Physics* 10, no. 23: 11647, 2010.
- 701 Eckhardt, S., Hermansen, O., Grythe, H., Fiebig, M., Stebel, K., Cassiani, M., Baecklund, A. and Stohl,  
 702 A.: The influence of cruise ship emissions on air pollution in Svalbard - a harbinger of a more polluted  
 703 Arctic?, *Atmospheric Chem. Phys.*, 13(16), 8401–8409, doi:<https://doi.org/10.5194/acp-13-8401-2013>,  
 704 2013.
- 705 Eckhardt, S., Quennehen, B., Olivieri, D. J. L., Berntsen, T. K., Cherian, R., Christensen, J. H., W. Collins  
 706 et al. "Current model capabilities for simulating black carbon and sulfate concentrations in the Arctic



- 707 atmosphere: a multi-model evaluation using a comprehensive measurement data set." *Atmospheric*  
 708 *Chemistry and Physics* 15, no. 16: 9413-9433, 2015.
- 709 Eleftheriadis, K., Vratolis, S. and Nyeki, S.: Aerosol black carbon in the European Arctic: Measurements  
 710 at Zeppelin station, Ny-Ålesund, Svalbard from 1998–2007, *Geophys. Res. Lett.*, 36(2),  
 711 doi:10.1029/2008GL035741, 2009.
- 712 Emerson, E. W., Katich, J. M., Schwarz, J. P., McMeeking, G. R. and Farmer, D. K.: Direct  
 713 Measurements of Dry and Wet Deposition of Black Carbon Over a Grassland, *J. Geophys. Res.*  
 714 *Atmospheres*, 123(21), 12,277-12,290, doi:10.1029/2018JD028954, 2018.
- 715 Feltracco, M., Barbaro, E., Kirchgeorg, T., Spolaor, A., Turetta, C., Zangrando, R., Barbante, C. and  
 716 Gambaro, A.: Free and combined L- and D-amino acids in Arctic aerosol, *Chemosphere*, 220, 412–421,  
 717 doi:10.1016/j.chemosphere.2018.12.147, 2019.
- 718 Feltracco, M., Barbaro, E., Tedeschi, S., Spolaor, A., Turetta, C., Vecchiato, M., Morabito, E.,  
 719 Zangrando, R., Barbante, C. and Gambaro, A.: Interannual variability of sugars in Arctic aerosol:  
 720 Biomass burning and biogenic inputs, *Sci. Total Environ.*, 706, 136089,  
 721 doi:10.1016/j.scitotenv.2019.136089, 2020.
- 722 Ferrero, L., Cappelletti, D., Busetto, M., Mazzola, M., Lupi, A., Lanconelli, C., Becagli, S., Traversi, R.,  
 723 Caiazza, L., Giardi, F., Moroni, B., Crocchianti, S., Fierz, M., Mocnik, G., Sangiorgi, G., Perrone, M.  
 724 G., Maturilli, M., Vitale, V., Udisti, R. and Bolzacchini, E.: Vertical profiles of aerosol and black carbon  
 725 in the Arctic: a seasonal phenomenology along two years (2011-2012) of field campaign, *Atmospheric*  
 726 *Chem. Phys.*, 16, 12601–12629, doi: 10.5194/acp-16-12601-2016, hdl:10013/epic.48736, 2016.
- 727 Flanner, M. G.: Arctic climate sensitivity to local black carbon, *J. Geophys. Res. Atmospheres*, 118(4),  
 728 1840–1851, doi:10.1002/jgrd.50176, 2013.
- 729 Flanner, M. G., Zender, C. S., Randerson, J. T. and Rasch, P. J.: Present-day climate forcing and response  
 730 from black carbon in snow, *J. Geophys. Res. Atmospheres*, 112(D11), doi:10.1029/2006JD008003,  
 731 2007.
- 732 Forsström, S., Ström, J., Pedersen, C. A., Isaksson, E. and Gerland, S.: Elemental carbon distribution in  
 733 Svalbard snow, *J. Geophys. Res. Atmospheres*, 114(D19), doi:10.1029/2008JD011480, 2009.
- 734 Forsström, S., Isaksson, E., Skeie, R. B., Ström, J., Pedersen, C. A., Hudson, S. R., Berntsen, T. K.,  
 735 Lihavainen, H., Godtliebsen, F. and Gerland, S.: Elemental carbon measurements in European Arctic  
 736 snowpacks, *J. Geophys. Res. Atmospheres*, 118(24), 13,614-13,627, doi:10.1002/2013JD019886, 2013.
- 737 Gallet JC, Björkman M, Larose C, Luks B., Martma T. and Zdanowics C. (eds). Protocols and  
 738 recommendations for the measurement of snow physical properties, and sampling of snow for black  
 739 carbon, water isotopes, major ions and micro-organisms. Norwegian Polar Institute. Kortrapport / Brief  
 740 Report no. 046, ISBN 978-82-7666-415-7 (printed), www.npolar.no, 2018.
- 741 Gogoi, M. M., Babu, S. S., Moorthy, K. K., Thakur, R. C., Chaubey, J. P. and Nair, V. S.: Aerosol black  
 742 carbon over Svalbard regions of Arctic, *Polar Sci.*, 10(1), 60–70, doi:10.1016/j.polar.2015.11.001, 2016.
- 743 Gundel, L. A., Dod, R. L., Rosen, H. and Novakov, T.: Relationship between optical attenuation and  
 744 black carbon concentration for ambient and source particles, Lawrence Berkeley Lab., CA (USA).  
 745 [online] Available from: <https://www.osti.gov/biblio/5653266> (Accessed 7 May 2020), 1983.



- 746 Hadley, O. L. and Kirchstetter, T. W.: Black-carbon reduction of snow albedo, *Nat. Clim. Change*, 2(6),  
 747 437–440, doi:10.1038/nclimate1433, 2012.
- 748 Hansen, J. and Nazarenko, L.: Soot climate forcing via snow and ice albedos, *Proc. Natl. Acad. Sci.*,  
 749 101(2), 423–428, doi:10.1073/pnas.2237157100, 2004.
- 750 Ingersoll, G.P., Don Campbell, M. Alisa Mast, David W. Clow, Leora Nanus, and Brent Frakes. 2009.  
 751 Snowpack Chemistry Monitoring Protocol for the Rocky Mountain Network; Narrative and Standard  
 752 Operating Procedures. United States Geological Service (USGS), Reston, Virginia. Administrative  
 753 Report, 2009
- 754 Jacobi, H.-W., Obleitner, F., Da Costa, S., Ginot, P., Eleftheriadis, K., Aas, W. and Zannata, M.:  
 755 Deposition of ionic species and black carbon to the Arctic snowpack: combining snow pit observations  
 756 with modeling, 10361-10377, doi:10.5194/acp-19-10361-2019, 2019.
- 757 Khan, A. L., Dierssen, H., Schwarz, J. P., Schmitt, C., Chlus, A., Hermanson, M., Painter, T. H. and  
 758 McKnight, D. M.: Impacts of coal dust from an active mine on the spectral reflectance of Arctic surface  
 759 snow in Svalbard, Norway, *J. Geophys. Res. Atmospheres*, 122(3), 1767–1778,  
 760 doi:10.1002/2016JD025757, 2017.
- 761 Laborde, M., Crippa, M., Tritscher, T., Jurányi, Z., Decarlo, P. F., Temime-Roussel, B., Marchand, N.,  
 762 Eckhardt, S., Stohl, A., Baltensperger, U., Prévôt, A. S. H., Weingartner, E. and Gysel, M.: Black  
 763 carbon physical properties and mixing state in the European megacity Paris, *Atmospheric Chem. Phys.*,  
 764 13(11), 5831–5856, doi:10.5194/acp-13-5831-2013, 2013.
- 765 Laj, P., Bigi, A., Rose, C., Andrews, E., Lund Myhre, C., Collaud Coen, M., Wiedensohler, A., Schultz,  
 766 M., Ogren, J. A., Fiebig, M., Glib, J., Mortier, A., Pandolfi, M., Petäjä, T., Kim, S.-W., Aas, W., Putaud,  
 767 J.-P., Mayol-Bracero, O., Keywood, M., Labrador, L., Aalto, P., Ahlberg, E., Alados Arboledas, L.,  
 768 Alastuey, A., Andrade, M., Artíñano, B., Ausmeel, S., Arsov, T., Asmi, E., Backman, J., Baltensperger,  
 769 U., Bastian, S., Bath, O., Beukes, J. P., Brem, B. T., Bukowiecki, N., Conil, S., Couret, C., Day, D.,  
 770 Dayantolis, W., Degorska, A., Santos, S. M. D., Eleftheriadis, K., Fethatzis, P., Favez, O., Flentje, H.,  
 771 Gini, M. I., Gregorič, A., Gysel-Beer, M., Hallar, G. A., Hand, J., Hoffer, A., Hueglin, C., Hooda, R. K.,  
 772 Hyvärinen, A., Kalapov, I., Kalivitis, N., Kasper-Giebl, A., Kim, J. E., Kouvarakis, G., Kranjc, I.,  
 773 Krejci, R., Kulmala, M., Labuschagne, C., Lee, H.-J., Lihavainen, H., Lin, N.-H., Löschau, G., Luoma,  
 774 K., Marinoni, A., Meinhardt, F., Merkel, M., Metzger, J.-M., Mihalopoulos, N., Nguyen, N. A.,  
 775 Ondracek, J., Pérez, N., Perrone, M. R., Petit, J.-E., Picard, D., Pichon, J.-M., Pont, V., Prats, N., Prenni,  
 776 A., Reisen, F., Romano, S., Sellegri, K., Sharma, S., Schauer, G., Sheridan, P., Sherman, J. P., Schütze,  
 777 M., Schwerin, A., Sohmer, R., Sorribas, M., Steinbacher, M., Sun, J., Titos, G., Tokzko, B., et al.: A  
 778 global analysis of climate-relevant aerosol properties retrieved from the network of GAW near-surface  
 779 observatories, *Atmospheric Meas. Tech. Discuss.*, 1–70, doi:https://doi.org/10.5194/amt-2019-499,  
 780 2020.
- 781 Law, K. S. and Stohl, A.: Arctic Air Pollution: Origins and Impacts, *Science*, 315(5818), 1537–1540,  
 782 doi:10.1126/science.1137695, 2007.
- 783 Lim, S., Fain, X., Zannata, M., Cozic, J., Jaffrezo, J. L., Ginot, P. and Laj, P.: Refractory black carbon  
 784 mass concentrations in snow and ice : method evaluation and inter-comparison with elemental carbon  
 785 measurement, *Atmospheric Meas. Tech.*, 7(10), 3307–3324, doi:10.5194/amt-7-3307-2014, 2014.
- 786 Liu, J., Fan, S., Horowitz, L. W. and Levy, H.: Evaluation of factors controlling long-range transport of  
 787 black carbon to the Arctic, *J. Geophys. Res. Atmospheres*, 116(D4), doi:10.1029/2010JD015145, 2011.



- 788 Long J.A.. jtools: Analysis and Presentation of Social Scientific Data (2020). URL: [https://cran.r-](https://cran.r-project.org/package=jtools)  
 789 [project.org/package=jtools](https://cran.r-project.org/package=jtools)
- 790 Lupi, A., Busetto, M., Becagli, S., Giardi, F., Lanconelli, C., Mazzola, M., Udisti, R., Hansson, H.-C.,  
 791 Henning, T., Petkov, B., Ström, J., Krejci, R., Tunved, P., Viola, A. P. and Vitale, V.: Multi-seasonal  
 792 ultrafine aerosol particle number concentration measurements at the Gruebadet observatory, Ny-  
 793 Ålesund, Svalbard Islands, *Rendiconti Lincei*, 27(1), 59–71, doi:10.1007/s12210-016-0532-8, 2016.
- 794 Maturilli, M., Herber, A. and König-Langlo, G.: Climatology and Time Series of Surface Meteorology in  
 795 Ny-Ålesund, Svalbard, *Earth Syst. Sci. Data*, 5, 155–163, doi:Maturilli, M. ORCID:  
 796 <https://orcid.org/0000-0001-6818-7383> <<https://orcid.org/0000-0001-6818-7383>>, Herber, A. and  
 797 König-Langlo, G. (2013) Climatology and Time Series of Surface Meteorology in Ny-Ålesund,  
 798 Svalbard , *Earth System Science Data*, 5 , pp. 155-163 . doi:[https://doi.org/10.5194/essd-5-](https://doi.org/10.5194/essd-5-155-2013)  
 799 [155-2013](https://doi.org/10.5194/essd-5-155-2013) <<https://doi.org/10.5194/essd-5-155-2013>> , hdl:10013/epic.41355, 2013.
- 800 Maturilli, M., Herber, A. and König-Langlo, G.: Surface radiation climatology for Ny-Ålesund, Svalbard  
 801 (78.9° N), basic observations for trend detection, *Theor. Appl. Climatol.*, 120(1), 331–339,  
 802 doi:10.1007/s00704-014-1173-4, 2015.
- 803 Maturilli, M., Hanssen-Bauer, I., Neuber, R., Rex, M. and Edvardsen, K.: The Atmosphere Above Ny-  
 804 Ålesund: Climate and Global Warming, Ozone and Surface UV Radiation, in *The Ecosystem of*  
 805 *Kongsfjorden, Svalbard*, edited by H. Hop and C. Wiencke, pp. 23–46, Springer International  
 806 Publishing, Cham., 2019.
- 807 Meinander, O.; Heikkinen, E.; Aurela, M.; Hyvärinen, A. Sampling, Filtering, and Analysis Protocols to  
 808 Detect Black Carbon, Organic Carbon, and Total Carbon in Seasonal Surface Snow in an Urban  
 809 Background and Arctic Finland (>60° N). *Atmosphere* 2020, 11, 923.  
 810 <https://doi.org/10.3390/atmos11090923>, 2020a.
- 811 Moosmüller, H., Chakrabarty, R. K. and Arnott, W. P.: Aerosol light absorption and its measurement: A  
 812 review, *J. Quant. Spectrosc. Radiat. Transf.*, 110(11), 844–878, doi:10.1016/j.jqsrt.2009.02.035, 2009.
- 813 Mori, T., Goto-Azuma, K., Kondo, Y., Ogawa-Tsukagawa, Y., Miura, K., Hirabayashi, M., Oshima, N.,  
 814 Koike, M., Kupiainen, K., Moteki, N., Ohata, S., Sinha, P. R., Sugiura, K., Aoki, T., Schneebeli, M.,  
 815 Steffen, K., Sato, A., Tsushima, A., Makarov, V., Omiya, S., Sugimoto, A., Takano, S. and Nagatsuka,  
 816 N.: Black Carbon and Inorganic Aerosols in Arctic Snowpack, *J. Geophys. Res. Atmospheres*, 124(23),  
 817 13325–13356, doi:10.1029/2019JD030623, 2019.
- 818 Moroni, B., Becagli, S., Bolzacchini, E., Busetto, M., Cappelletti, D., Crocchianti, S., Ferrero, L., Frosini,  
 819 D., Lanconelli, C., Lupi, A., Maturilli, M., Mazzola, M., Perrone, M. G., Sangiorgi, G., Traversi, R.,  
 820 Udisti, R., Viola, A. and Vitale, V.: Vertical Profiles and Chemical Properties of Aerosol Particles upon  
 821 Ny-Ålesund (Svalbard Islands), *Adv. Meteorol.*, 2015, e292081,  
 822 doi:<https://doi.org/10.1155/2015/292081>, 2015.
- 823 Moroni, B., Arnalds, O., Dagsson-Waldhauserová, P., Crocchianti, S., Vivani, R. and Cappelletti, D.:  
 824 Mineralogical and Chemical Records of Icelandic Dust Sources Upon Ny-Ålesund (Svalbard Islands),  
 825 *Front. Earth Sci.*, 6, doi:10.3389/feart.2018.00187, 2018.
- 826 Moroni, B., Ritter, C., Crocchianti, S., Markowicz, K., Mazzola, M., Becagli, S., et al.. Individual particle  
 827 characteristics, optical properties and evolution of an extreme long-range transported biomass burning



- 828 event in the European Arctic (Ny-Ålesund, Svalbard Islands). *Journal of Geophysical Research:*  
 829 *Atmospheres*, 125, e2019JD031535. <https://doi.org/10.1029/2019JD031535>, 2020.  
 830
- 831 Motos, G., Schmale, J., Corbin, J. C., Modini, R. L., Karlen, N., Bertò, M., Baltensperger, U. and Gysel-  
 832 Beer, M.: Cloud droplet activation properties and scavenged fraction of black carbon in liquid-phase  
 833 clouds at the high-alpine research station Jungfrauoch (3580&thinsp;m&thinsp;a.s.l.), *Atmospheric*  
 834 *Chem. Phys.*, 19(6), 3833–3855, doi:<https://doi.org/10.5194/acp-19-3833-2019>, 2019.
- 835 Osmont, D., Wendl, I. A., Schmidely, L., Sigl, M., Vega, C. P., Isaksson, E. and Schwikowski, M.: An  
 836 800-year high-resolution black carbon ice core record from Lomonosovfonna, Svalbard, *Atmospheric*  
 837 *Chem. Phys.*, 18(17), 12777–12795, doi:<https://doi.org/10.5194/acp-18-12777-2018>, 2018.
- 838 Pedersen, C. A., Gallet, J.-C., Ström, J., Gerland, S., Hudson, S. R., Forsström, S., Isaksson, E. and  
 839 Berntsen, T. K.: In situ observations of black carbon in snow and the corresponding spectral surface  
 840 albedo reduction, *J. Geophys. Res. Atmospheres*, 120(4), 1476–1489, 2015.
- 841 Petzold, A., Ogren, J. A., Fiebig, M., Laj, P., Li, S.-M., Baltensperger, U., Holzer-Popp, T., Kinne, S.,  
 842 Pappalardo, G., Sugimoto, N., Wehrli, C., Wiedensohler, A. and Zhang, X.-Y.: Recommendations for  
 843 reporting “black carbon” measurements, *Atmospheric Chem. Phys.*, 13(16), 8365–8379,  
 844 doi:<https://doi.org/10.5194/acp-13-8365-2013>, 2013.
- 845 R Core Team. R: A language and environment for statistical computing. R Foundation for Statistical  
 846 Computing, Vienna, Austria, (2020). URL: <https://www.R-project.org/>
- 847 Ruppel, M. M., Soares, J., Gallet, J.-C., Isaksson, E., Martma, T., Svensson, J., Kohler, J., Pedersen, C.  
 848 A., Manninen, S., Korhola, A. and Ström, J.: Do contemporary (1980–2015) emissions determine the  
 849 elemental carbon deposition trend at Holtedahlfonna glacier, Svalbard?, *Atmospheric Chem. Phys.*,  
 850 17(20), 12779–12795, doi:<https://doi.org/10.5194/acp-17-12779-2017>, 2017.
- 851 Scalabrin, E., Zangrando, R., Barbaro, E., Kehrwald, N. M., Gabrieli, J., Barbante, C. and Gambaro, A.:  
 852 Amino acids in Arctic aerosols, *Atmospheric Chem. Phys.*, 12(21), 10453–10463,  
 853 doi:<https://doi.org/10.5194/acp-12-10453-2012>, 2012.
- 854 Schmale, J., Arnold, S. R., Law, K. S., Thorp, T., Anenberg, S., Simpson, W. R., Mao, J. and Pratt, K. A.:  
 855 Local Arctic Air Pollution: A Neglected but Serious Problem, *Earths Future*, 6(10), 1385–1412,  
 856 doi:[10.1029/2018EF000952](https://doi.org/10.1029/2018EF000952), 2018.
- 857 Schwarz, J. P., Gao, R. S., Perring, A. E., Spackman, J. R. and Fahey, D. W.: Black carbon aerosol size in  
 858 snow, *Sci. Rep.*, 3(1), 1–5, doi:[10.1038/srep01356](https://doi.org/10.1038/srep01356), 2013.
- 859 Screen, J. A. and Simmonds, I.: The central role of diminishing sea ice in recent Arctic temperature  
 860 amplification, *Nature*, 464(7293), 1334–1337, doi:[10.1038/nature09051](https://doi.org/10.1038/nature09051), 2010.
- 861 Segura, S., Estellés, V., Titos Vela, G., Lyamani, H., Utrilla Navarro, P., Zotter, P., Prévot, A. S. H.,  
 862 Močnik, G., Alados-Arboledas, L. and Martínez-Lozano, J. A.: Determination and analysis of in situ  
 863 spectral aerosol optical properties by a multi-instrumental approach, , doi:[10.5194/amt-7-2373-2014](https://doi.org/10.5194/amt-7-2373-2014),  
 864 2014.
- 865 Serreze, M. C. and Barry, R. G.: Processes and impacts of Arctic amplification: A research synthesis,  
 866 *Glob. Planet. Change*, 77(1), 85–96, doi:[10.1016/j.gloplacha.2011.03.004](https://doi.org/10.1016/j.gloplacha.2011.03.004), 2011.





- 867 Sharma, S., W. Richard Leaitch, Lin Huang, Daniel Veber, Felicia Kolonjari, Wendy Zhang. An  
 868 evaluation of three methods for measuring black carbon in Alert, Canada. *Atmos. Chem. Phys.*, 17,  
 869 15225–15243, <https://doi.org/10.5194/acp-17-15225-2017>, 2017.
- 870 Sinha, P. R., Y. Kondo, M. Koike, J. Ogren, A. Jefferson, T. Barrett, R. Sheesley, S. Ohata, N. Moteki, H.  
 871 Coe, D. Liu, M. Irwin, P. Tunved, P. K. Quinn, and Y. Zhao, Evaluation of ground-based black carbon  
 872 measurements by filter-based photometers at two Arctic sites, *J. Geophys. Res.*, 122,  
 873 doi:10.1002/2016JJD025843, 2017.
- 874 Sinha, P. R., Kondo, Y., Goto-Azuma, K., Tsukagawa, Y., Fukuda, K., Koike, M., Ohata, S., Moteki, N.,  
 875 Mori, T., Oshima, N., Førland, E. J., Irwin, M., Gallet, J.-C. and Pedersen, C. A.: Seasonal Progression  
 876 of the Deposition of Black Carbon by Snowfall at Ny-Ålesund, Spitsbergen: Deposition of Black  
 877 Carbon in Spitsbergen, *J. Geophys. Res. Atmospheres*, 123(2), 997–1016, doi:10.1002/2017JD028027,  
 878 2018.
- 879 Skiles, S. M. and Painter, T. H.: Toward Understanding Direct Absorption and Grain Size Feedbacks by  
 880 Dust Radiative Forcing in Snow With Coupled Snow Physical and Radiative Transfer Modeling, *Water*  
 881 *Resour. Res.*, 55(8), 7362–7378, doi:10.1029/2018WR024573, 2019.
- 882 Skiles, S. M., Flanner, M., Cook, J. M., Dumont, M. and Painter, T. H.: Radiative forcing by light-  
 883 absorbing particles in snow, *Nat. Clim. Change*, 8(11), 964–971, doi:10.1038/s41558-018-0296-5, 2018.
- 884 Spolaor, A., Angot, H., Roman, M., Dommergue, A., Scarchilli, C., Vardè, M., Del Guasta, M., Pedeli,  
 885 X., Varin, C., Sprovieri, F., Magand, O., Legrand, M., Barbante, C. and Cairns, W. R. L.: Feedback  
 886 mechanisms between snow and atmospheric mercury: Results and observations from field campaigns on  
 887 the Antarctic plateau, *Chemosphere*, 197, 306–317, doi:10.1016/j.chemosphere.2017.12.180, 2018.
- 888 Spolaor, A., Barbaro, E., Cappelletti, D., Turetta, C., Mazzola, M., Giardi, F., Björkman, M. P.,  
 889 Lucchetta, F., Dallo, F., Pfaffhuber, K. A., Angot, H., Dommergue, A., Maturilli, M., Saiz-Lopez, A.,  
 890 Barbante, C. and Cairns, W. R. L.: Diurnal cycle of iodine, bromine, and mercury concentrations in  
 891 Svalbard surface snow, *Atmospheric Chem. Phys.*, 19(20), 13325–13339,  
 892 doi:<https://doi.org/10.5194/acp-19-13325-2019>, 2019.
- 893 Stephens, M., Turner, N. and Sandberg, J.: Particle identification by laser-induced incandescence in a  
 894 solid-state laser cavity, *Appl. Opt.*, 42(19), 3726–3736, doi:10.1364/AO.42.003726, 2003.
- 895 Stohl, A., Klimont, Z., Eckhardt, S., Kupiainen, K., Shevchenko, V. P., Kopeikin, V. M., and Novigatsky,  
 896 A. N.: "Black carbon in the Arctic: the underestimated role of gas flaring and residential combustion  
 897 emissions.", 2013.
- 898 Tunved, P., Ström, J. and Krejci, R.: Arctic aerosol life cycle: linking aerosol size distributions observed  
 899 between 2000 and 2010 with air mass transport and precipitation at Zeppelin station, Ny-Ålesund,  
 900 Svalbard, *Atmospheric Chem. Phys.*, 13(7), 3643–3660, doi:<https://doi.org/10.5194/acp-13-3643-2013>,  
 901 2013.
- 902 Vecchiato, M., Barbaro, E., Spolaor, A., Burgay, F., Barbante, C., Piazza, R. and Gambaro, A.,  
 903 Fragrances and PAHs in snow and seawater of Ny-Ålesund (Svalbard): Local and long-range  
 904 contamination. *Environmental Pollution* 242, 1740–1747,  
 905 doi:<https://doi.org/10.1016/j.envpol.2018.07.095> (2018).





- 906 Weingartner, E., Saathoff, H., Schnaiter, M., Streit, N., Bitnar, B. and Baltensperger, U.: Absorption of  
 907 light by soot particles: determination of the absorption coefficient by means of aethalometers, *J. Aerosol*  
 908 *Sci.*, 34(10), 1445–1463, doi:10.1016/S0021-8502(03)00359-8, 2003.
- 909 Wendl, I. A., Menking, J. A., Färber, R., Gysel, M., Kaspari, S. D., Laborde, M. J. G. and Schwikowski,  
 910 M.: Optimized method for black carbon analysis in ice and snow using the Single Particle Soot  
 911 Photometer, *Atmospheric Meas. Tech.*, 7, 2667–2681, doi:10.5194/amt-7-2667-2014, 2014.
- 912 Yasunari, T. J., Tan, Q., Lau, K.-M., Bonasoni, P., Marinoni, A., Laj, P., Ménégos, M., Takemura, T. and  
 913 Chin, M.: Estimated range of black carbon dry deposition and the related snow albedo reduction over  
 914 Himalayan glaciers during dry pre-monsoon periods, *Atmos. Environ.*, 78, 259–267,  
 915 doi:10.1016/j.atmosenv.2012.03.031, 2013.
- 916 Zanatta, M., Gysel, M., Bukowiecki, N., Müller, T., Weingartner, E., Areskoug, H., Fiebig, M., Yttri, K.  
 917 E., Mihalopoulos, N., Kouvarakis, G., Beddows, D., Harrison, R. M., Cavalli, F., Putaud, J. P., Spindler,  
 918 G., Wiedensohler, A., Alastuey, A., Pandolfi, M., Sellegri, K., Swietlicki, E., Jaffrezo, J. L.,  
 919 Baltensperger, U. and Laj, P.: A European aerosol phenomenology-5: Climatology of black carbon  
 920 optical properties at 9 regional background sites across Europe, *Atmos. Environ.*, 145, 346–364,  
 921 doi:10.1016/j.atmosenv.2016.09.035, 2016.
- 922 Zanatta, M., Laj, P., Gysel, M., Baltensperger, U., Vratolis, S., Eleftheriadis, K., Kondo, Y., Dubuisson,  
 923 P., Winiarek, V., Kazadzis, S., Tunved, P. and Jacobi, H.-W.: Effects of mixing state on optical and  
 924 radiative properties of black carbon in the European Arctic, *Atmospheric Chem. Phys.*, 18(19), 14037–  
 925 14057, doi:https://doi.org/10.5194/acp-18-14037-2018, 2018.
- 926 Zangrando, R., Barbaro, E., Zennaro, P., Rossi, S., Kehrwald, N. M., Gabrieli, J., Barbante, C. and  
 927 Gambaro, A.: Molecular Markers of Biomass Burning in Arctic Aerosols, *Environ. Sci. Technol.*,  
 928 47(15), 8565–8574, doi:10.1021/es400125r, 2013.